

UDC 548.313:611.018.46.085.23.017.6

Spreading and proliferation of cultured rat bone marrow stromal cells on the surface of bioactive glass ceramics

V. V. Kiroshka¹, O. V. Savvova², Yu. O. Bozhkova¹, I. V. Tamarina¹, A. I. Fesenko²

¹ Institute for Problems of Cryobiology and Cryomedicine, NAS of Ukraine
23, Pereyaslavskaya Str., Kharkiv, Ukraine, 61015

² National Technical University “Kharkiv Polytechnic Institute”
2, Kyrpychova str., Kharkiv, Ukraine, 61002
alicefromwl@gmail.com

Aim. To study spreading profile, cytoskeleton structure organization, and proliferation of bone marrow stromal cells in the course of cultivation on the glass-crystalline material (GCM) surfaces, with different chemical composition and solubility. **Methods.** GCMs with different CaO: P₂O₅ ratios were used. The actins cytoskeleton in cells was visualized using fluorescent TRITC-conjugated phalloidin. Cell proliferation was studied using MTT test. **Results.** The cell cultivation on highly soluble B series GCM (Ca/P = 5 superficial ratio) led to appearance of fibroblast-like cells, the actin cytoskeleton filaments of which were uniformly distributed within cytoplasm. In this case, proliferation dynamics was similar to that] under cultivation on plastic. Ca/P ratio reduction on the surfaces of A and C series of GCMs to 1.4 ÷ 2.58 resulted in a decrease of spreading area and proliferation index (up to 2–3 times) relative to the control. **Conclusions.** Main factors, determining the cells interaction behavior with GCM are the materials solubility and Ca/P superficial ratio.

Keywords: glass-crystalline materials, bone marrow stromal cells.

New possibilities for injured organs and tissues recovery are provided with one of the most up-to-date interdisciplinary area of medicine, namely tissue engineering. It is based on the synthesis of new bioactive materials, with a range of chemical properties that aimed to enhance the treatment efficiency, enhance regeneration or substitute damaged tissues and organs [1]. Bio-reactive calcium phosphate scaffolds with cer-

tain CaO/P₂O₅ ratio such as glass, ceramics and glass-ceramic materials (GCM) are widely used for arthroplasty nowadays. GCMs based on crystalline calcium phosphate (CP) are the most promising for the orthopedic and dental implants creation [2, 3, 4].

GCMs are much more durable and fraction-resistant in comparison to hydroxyapatite ceramics, which is determined by their crypto-

© 2017 V. V. Kiroshka *et al.*; Published by the Institute of Molecular Biology and Genetics, NAS of Ukraine on behalf of Biopolymers and Cell. This is an Open Access article distributed under the terms of the Creative Commons Attribution License (<http://creativecommons.org/licenses/by/4.0/>), which permits unrestricted reuse, distribution, and reproduction in any medium, provided the original work is properly cited

crystalline structure (crystal size varies from 0.5 to 1.0 μm) [5]. In the presence of biological fluids the surface dissolution, sedimentation and ion exchange occur on GCM, leading to the formation of biologically equivalent hydroxyapatite layer (HA) [6]. The extracellular matrix proteoglycans and GAGs interactions with the GCM inorganic superficial components lead to their inclusion in the polycrystalline HA layer and further on, to ontogenesis induction. The HA layer structure and composition are determined by the calcium and phosphate oxides equilibrium on the GCM surface, availability of the HA crystal nucleation centers and solubility of the material, providing the calcium and phosphate ions diffusion into biological media.

The cell response is determined by the chemical composition, surface roughness [7] porosity [8], topography, grain size and crystallinity of the scaffolds [9]. However, the exact mechanism of interactions between the ionic dissolution products in such materials and human cells is not fully understood, which has prompted considerable research work on the biomaterials during the last decade.

The most promising biological component in the bio-engineering constructions are stromal cells (SC), derived from bone marrow (BMSC). BMSC are more “multitasking”, unlike SC from other sources, they are capable to differentiate into the tissues of both mesenchymal and non-mesenchymal origin [10, 11]. The analysis of the spreading, cytoskeleton structure, proliferation dynamics of BMSC during cultivation on GCM with determined physical and chemical characteristics is one of the most up-to-date models to study cell interactions whilst the tissue formation *in vitro* and *in vivo* [12].

This work is aimed at studying the spreading properties, cytoskeleton structure, proliferation of BMSC under the cultivation on GCM of varying chemical composition and solubility.

Materials and Methods

GCM, obtained on the base of calcium silicon phosphate glasses system $\text{Na}_2\text{O} - \text{K}_2\text{O} - \text{Li}_2\text{O} - \text{MgO} - \text{CaO} - \text{ZnO} - \text{ZrO}_2 - \text{TiO}_2 - \text{Al}_2\text{O}_3 - \text{B}_2\text{O}_3 - \text{P}_2\text{O}_5 - \text{SiO}_2$ with different ratios of $\text{CaO}/\text{P}_2\text{O}_5$ (1.5; 2.3; 4) have been used. GCM were melt under 1250 – 1450 $^\circ\text{C}$ in corundum crucibles with further cooling on the metal sheet. Phase composition of GCM was chosen for durability purpose with resistive crystalline phase (HA ($\text{Ca}_5(\text{PO}_4)_3\text{OH}$ (17 \div 30 v. %)), and for bioactivity purpose with resorption crystalline phase (rhenanite $\beta\text{-NaCaPO}_4$ (23 v. %) and carbonatefluorine-hydroxyapatite $\text{Ca}_5(\text{PO}_4)_3\text{CO}_3 \text{F}_{1,5}(\text{OH})_{0,5}$ (42 v. %)).

Formation of apatite-like layer on the surface of designed materials was determined *in vivo* with the model of biological fluid (MBF) according to ISO 10993-14:2001. MBF containing TRIS and HCL, Na^+ , K^+ , Mg^{2+} cations, Cl^- , HCO_3^{2-} , HPO_4^{2-} anions was used to recreate conditions in a living organism (*in vivo*) [13]. To determine solubility, an increase in the weight (%) of studied samples was measured within incubation in MBF at 37 $^\circ\text{C}$ for 180 days.

Elemental composition of a sample surface was determined with an electron-probe microanalysis on the scanning electron microscope *REM Tescan Mira 3LMU* with the energy dispersive spectrometer *Oxford X-max 80mm*.

Rat bone marrow stromal cell isolation and culture. BMSC were isolated from the

femurs and tibias of young male Wistar rats (75–100 g body weight). All manipulations with animals were carried out in accordance with the requirements of the Bioethics Committee of the Institute for Problems of Cryobiology and Cryomedicine of the National Academy of Sciences of Ukraine and the “General Principles of Experiments on Animals” accepted by the 1st National Congress on Bioethics (Kiev, Ukraine, 2004). These principles are based on the theses of European Convention for the Protection of Vertebrate Animals Used for Experimental and Other Scientific Purposes (Strasbourg, France (1986)). The culture medium consisted of Dulbecco’s modified Eagle’s minimal essential medium (DMEM-F12) (Sigma-Aldrich, USA), supplemented with 100 U/ml of penicillin (Sandoz GmbH, Austria), 100 mg/ml of streptomycin («Kyivmedpreparat», Ukraine), 1.25 mg/ml of gentamicin (Darnitsa, Ukraine), 0.5 mg/ml of amphotericin B (Sigma-Aldrich, USA) and 15 % fetal calf serum (FCS). Bone marrow was flushed out under sterile conditions with 10 mL of culture media using a syringe and 18-gauge needle. The collected marrow was homogenized and centrifuged at 500 g for 5 min. The resulting cell pellets were re-suspended in 5 ml of culture medium and transferred to T-25 cell culture flasks. The medium was changed after 48 h to remove non-adherent cells and then changed every 2–3 days over the course of each subculture period [14]. When the cell monolayer reached 80 % confluence, the cells were removed enzymatically (with a solution containing 0.01 % trypsin and 0.05 % ethylenediaminetetraacetic acid (EDTA) (Gibco, USA)) and subcultured at a 1:3 ratio. The cells were passaged every

5–7 days until the desired cell number was obtained for further cell seeding. All flasks were incubated under standard cell culture conditions (37 °C, 5 % CO₂, 100 % relative humidity) in a CO₂ incubator (Sanyo, Japan). The BMSC were used at the 3rd or 4th passage for all experiments [15].

BMSC seeding. Samples of GCM 1.2×1.2×1.0 cm³ were preliminary sterilized with UV radiation $\lambda=254$ nm for 30 min, then placed in the 24 well plate and incubated in culture medium during 24 h at 37 °C, 5 % CO₂ and 100 % humidity. That was followed by the media replacement and cell seeding. Cell concentration in each well of 24-well plate was 0.7-1.0×10⁵ cells/ml. GCM with various CaO/P₂O₅ ratios were used (tabl.1) and were absent in control wells.

Evaluation of cytoskeleton organization. The actin cytoskeleton of BMSC was visualized by fluorescent staining after 2-day cultivation on GCM. The samples were fixed in 4 % paraformaldehyde for 20 min, with subsequent staining with TRITC-conjugated phalloidin (1:1000). The actin cytoskeleton was examined using the Carl Zeiss Axio Observer Z1 fluorescence microscope; images were processed using the corresponding software program.

Morphological analysis. The intravital morphology of cells after 2-days cultivation on GCM was studied using an inverted fluorescence microscope (Am Scope, model XYL-403). The cell spreading areas and cell perimeters were determined using Axio Vision image analysis software. The cell shape index (SI) was calculated using the following formula: $SI = 4\pi \times S/P^2$, where S is the BMSC spreading area and P is the BMSC perimeter. A value of the cell SI close to unity indicated the presence of spherical cells [16].

Cell proliferation analysis. Cell proliferation was studied after 1, 3, and 5 days using MTT test [17]. 5 mg/mL solution of MTT in DMEM-F12 medium (Sigma-Aldrich, USA) was added to the cells and incubated for 4 h at 37 °C. The intracellular formazan crystals were dissolved by the addition of dimethylsulfoxide, and the absorption was measured at 570 nm using an SF-4 spectrophotometer (LOMO, Russia). The numbers of cells in the samples were calculated from their absorption values, using a calibration curve plotted for the cell concentrations $(2.5, 5, 10, 20) \times 10^4$ [18]. The proliferation index was determined as the ratio of the number of metabolically active cells and the number of cells initially inoculated, according to the following formula: $I = [A/A_0] \times 100 \%$, where A_0 is the initial cell concentration, and A is the cell concentration at the current time [19].

Statistical analysis. The reproducibility of the data was demonstrated by analyzing all experimental groups as biological triplicates, and all control groups as biological duplicates. Data are presented as mean \pm standard error of the mean (SEM). Student's t-test was used for statistical analysis. Data were considered significantly different if $P < 0.05$. The means and the standard deviations were reported.

Results and Discussion

GCM solubility and MBF components sedimentation during 3–180 days of incubation are presented in Fig.1 Apparently, on the 3-d day of incubation in MBF [the] mass loss was similar for all designed GCM and varied from 0.05 to 0.1 %. An increase in the incubation time up to 30 ÷ 60 days led to the exponential mass gain. After 90 days of incubation, the mass gain profile changed to linear dependence, which reflects intensification of the MBF components sedimentation. Notably, on the [180th] day the mass gain for A series GCM was 5 to 7 times lower, compared to B and C series respectively.

As it appears from the data (Table), Si concentration decreases along with the Ca and P concentrations increase in the superficial layer at the materials exposition to MBF. This fact proves the simultaneous formation of silica gel and calcium phosphate layer on the GCM surface and indicates a potential apatite-forming process. The presence of silicon in superficial layers provides the formation of silanols, which are effective centers for HA nucleation [20]. It has to be emphasized, that under incubation in MBF Ca and P resorption on GCM surfaces in the B and C series was sig-

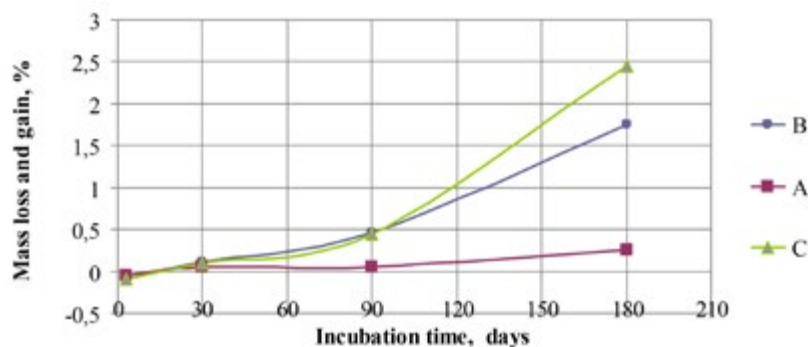


Fig. 1. GCM solubility and kinetics of MBF components sedimentation during 180-day incubation of the samples of A B C series.

The surface rigidity values ((R_s)) and chemical composition before and after 180-day incubation are presented in Table.

Table 1. Superficial morphology and chemical composition before and after incubation in MBF.

Physical-chemical properties		Glass crystalline materials (GCM)		
		A series	B series	C series
Ratio of CaO: P ₂ O ₅ in glass structure		4.0	2.3	1.5
Mass increase in MBF (180 days), %		0.33	1.8	2.3
Characteristics of calcium phosphate crystals, ≤ 1 μm		Ca ₅ (PO ₄) ₃ OH	Ca ₅ (PO ₄) ₃ CO ₃ F _{1.5} OH _{0.5}	β-NaCaPO ₄ Ca ₅ (PO ₄) ₃ OH
Rigidity of the surface (R _a), μm		6.0	10.0	2.5
The atomic ratio of the elements on the surface	Ca: P (before soaking in MBF)	1.4	5.0	2.58
	Ca: P (after soaking in MBF)	0.87	1.6	0.82
	Si: Ca: P (before soaking in MBF)	1:0.93:0.66	1:0.4:0.08	1:0.5:0.2
	Si: Ca: P (after soaking in MBF)	1:2.54:2.9	1:4:2.5	1:6:7

nificantly higher comparing to the A series (Table). Herewith, rigidity of the surface (R_a) was 6.0; 10.0 and 2.5 μm for A, B and C series respectively, defined, obviously, by the structure and composition on the materials surfaces (Table).

To evaluate the cell behavior on the GCM under cultivation, the BMSC morphology, spreading area, cytoskeleton condition and proliferation dynamics were studied. As seen from Fig. 2A, when cultivated on plastic, the BMSC morphology varied from polygonal to spindle and fibroblast-like shapes with uniformly dispersed actin cytoskeleton microfilaments within cytoplasm. The BMSC shapes in contact with the B series GCM varied from polygonal to spindle like with multiple processes, e.g. were similar to control (shape indexes were 0.46±0.19, and 0.43±0.14 for B series and control respectively).

Thus, the actins cytoskeleton microfilaments in the B series GCM cultured cells were uniformly organized within the cells (Fig. 2, C). Notably, the cell spreading area values (Fig. 2, F) for the B series were comparable to those in control, whereas in GCM of A and

C series a significant area decrease was observed (2310.66±839.88, 1673.79±973.91 in the A, C series, and 4840.99±2274.40 in control, respectively). During cultivation on GCM of A (Fig. 2, B) and C series (Fig. 2, D) we found the round shaped and elongated rod-shaped cells with multiple processes. In such cells, the actin microfilaments were redistributed from periphery to the center. The proliferation analysis proved, that the BMSC growth dynamics on the B series GCM is comparable to control values, whereas it was 2-3 times lower for the A and C series (Fig. 1, G).

The results above indicate that the BMSC behavior under cultivation on GCM is determined by its physical and chemical properties (solubility, Ca and P resorption speed, CP crystals structure and components.). Thus, the form, spreading area, and proliferation profile data analysis of BMSC cultured on GCM revealed that only in case of the B series GCM the cell behavior was similar to that under cultivation on plastic (Fig. 2).

This fact, obviously, might be explained by the structure and atomic Ca to P ratio on the GCM surface. Notably, in our experiment, the

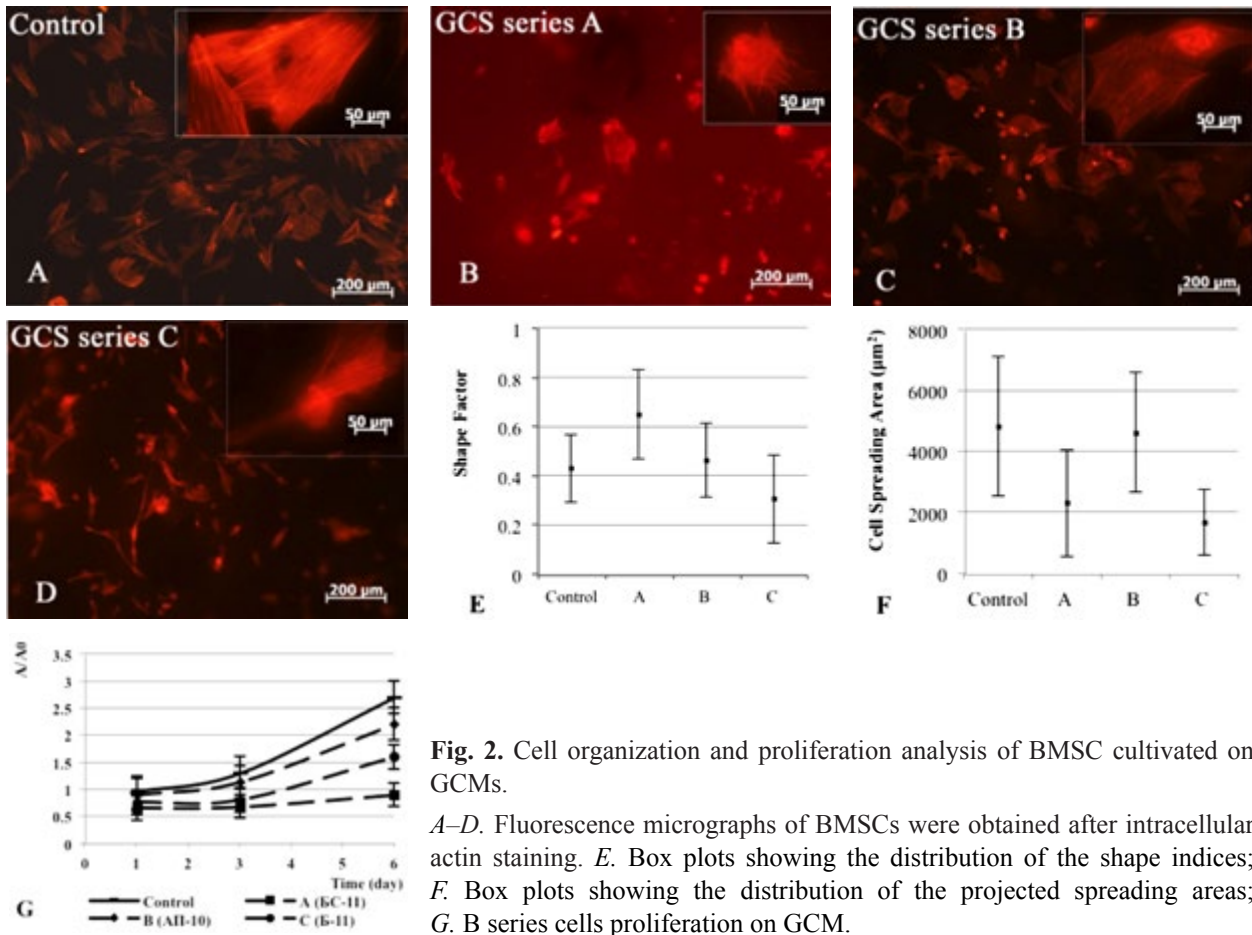


Fig. 2. Cell organization and proliferation analysis of BMSC cultivated on GCMs.

A–D. Fluorescence micrographs of BMSCs were obtained after intracellular actin staining. *E.* Box plots showing the distribution of the shape indices; *F.* Box plots showing the distribution of the projected spreading areas; *G.* B series cells proliferation on GCM.

surface rigidity is not a key determination factor of the BMSC behavior under cultivation. According to the literature data [21, 22] micro- and nanotopography of the growth surface determines the cell behavior under cultivation on extracellular matrixes. It was shown [23] that the cells, cultivated on the material with superficial rigidity 2000 nm, did not spread and detach. Comparing the data from fig. 2 and table 1, it can be seen, that the cell spreading on the GCM was observed for the material with the most rough surface ($R_a = 10 \mu\text{m}$). These experimental data allowed us to assume, that the determining factors of cell behavior

under cultivation on GCM are superficial Ca/P ratio and its solubility.

It is known [24] that GCM interactions with biological fluid result in the material dissolving, ions exchange and sedimentation of media components.

Comparing the data, presented in Table, one can notice that the B series GCM were highly soluble and had the highest Ca/P ratio value, resulting in the formation of CP crystals with non-stoichiometric ratio $\text{Ca/P} = 1.6$ that corresponds to a stoichiometry, specific for biogenic HA ($1.37 < 1.67 < 1.77$) [25, 26]. Besides, the chemical structure, solubility and resorption

speed in the B series GCM promoted such ionic exchange with MBF, which led to the carbon and fluorine ions (Table) insertions into the CP crystals structure. It is known, that fluorine ions replace the hydroxyl groups with consequent HA structure stabilization as in the case of full or partial OH⁻ replacement [27]. It was suggested [28] that the fluorine presence in the CP crystal structure provides the GCM surface stabilization in chemically active biologic media. In contrast, the presence of carbonate groups in HA structure leads to the deformations, micro stresses and defects in acrySTALLINE lattice [29]. It is shown that PO₄³⁻ replacement with carbonate groups results in a decrease of HA crystal size and crystallinity. In the model discussed, it is suggested that phosphate ions are replaced with carbonate ions, filling one Ca²⁺ and one hydroxyl vacancy [30]. Availability of such vacancies might lead to the Ca²⁺ presence on GCM surface, which are, in turn, the nucleation sites for tissues mineralization *in vivo*. It was shown that extracellular Ca²⁺ is actively involved in main cell reactions such as adhesion, spreading and following proliferation [31].

Two main probable mechanisms of Ca²⁺ influence on the cell-substrate interactions are considered [32]. First, specific cations may induce a conformational change in the integrins that favors ligand binding. Second, cation, ligand, and receptor may initially form a ternary complex, in which the ligand is bridged to the integrin through the cation, and the cation is then subsequently displaced from the ligand-binding site. In terms of experimental data, discussed above, it is expected that a sufficient quantity of calcium ions on the GCM surface in the B series contributed to the focal

adhesion zones and tight junctions formation, which, in turn, provided the cell spreading and proliferation comparable to a control. The BMSC characteristics under cultivation on GCM of the A and C series were qualitatively different. In these samples cell morphology was featured with round, rod-like cells with actin filaments accumulated in the perinuclear zone. The similar cytoskeleton structure, along with a small spreading area, under cultivation on GCM (Fig. 2) in these groups is due to an insufficient concentration of Ca²⁺ on the surface, which reduced the extracellular matrix substrate adhesion molecules affinity [33, 34]. As it appears from data (Table), the Ca/P ratio on the top of the A and C series GCM varies from 0.82 to 0.86, which is significantly lower compared to biogenic HA terminal meanings [25, 26]. This parameter was determinative for BMSC to the GCM surface interactions. It is shown, than Ca²⁺ are allosteric messengers, required for the adhesion receptors and superficial ligands binding, followed by cell spreading [35]. Hence, we can expect that insufficient Ca²⁺ concentration on the surface of the A and C series GCM determined the presence of unspread cells and a decrease in the proliferation dynamics of BMSC under cultivation. Comparing the data (Table) it should be noted that mass gain (2.3%) whilst incubation on the C series material in MBF resulted in the formation of sedimented CP layer with Ca/P=0.82. Due to an initial low Ca/P ratio in GCM structure, it may occur the sedimentation of sodium ions, that are comparable with calcium ions by an effective ionic radius. This is supported by the structural analysis of the sodium containing CP crystal (Tabl. 1). Therefore, initial GCM, along with high solubility, should have high

Ca/P ratio and CP crystals with Ca/P content within biogenic HA meanings ($\text{Ca/P} = 1,5 \div 1,67$) should be formed.

In conclusion, it must be admitted, that the physical and chemical characteristics of the GCM surface structure are the main factors, determining the cell behavior under cultivation *in vitro*. Cell cultivation on the highly soluble B series GCM ($\text{Ca/P}=5$ superficial ratio) led to the appearance of fibroblast-like cells with the actin cytoskeleton filaments uniformly distributed within cytoplasm. In this case, proliferation dynamics was similar to that during cultivation on plastic. The Ca/P ratio reduction up to $1.4 \div 2.58$ on the surfaces of A and C series GCMs resulted in 2-3-fold decrease of the cell spreading area and proliferation index relative to the control.

REFERENCES:

1. Lanza RP, Langer R, Vacanti JP. Principles of tissue engineering. 4th edition. Academic Press: Elsevier 2013, 1936 p.
2. Rezwan K, Chen QZ, Blaker JJ, Boccaccini AR. Biodegradable and bioactive porous polymer/inorganic composite scaffolds for bone tissue engineering. *Biomaterials*. 2006;**27**(18):3413-31.
3. Gerhardt L-C, Boccaccini AR. Bioactive glass and glass-ceramic scaffolds for bone tissue engineering. *Materials*. 2010; **3**(7): 3867-910.
4. Hoppe A, Güldal NS, Boccaccini AR. A review of the biological response to ionic dissolution products from bioactive glasses and glass-ceramics. *Biomaterials*. 2011;**32**(11):2757-74.
5. Sarkisov PD. Controlled glass crystallization as the basis for synthesis of multifunctional glass-crystalline materials. Moscow: D. Mendeleev University of Chemical Technology of Russia. 1997. 218 p.
6. Jones JR, Tsigkou O, Coates EE, Stevens MM, Polak JM, Hench LL. Extracellular matrix formation and mineralization on a phosphate-free porous bioactive glass scaffold using primary human osteoblast (HOB) cells. *Biomaterials*. 2007;**28**(9):1653-63.
7. Gough JE, Notingher I, Hench LL. Osteoblast attachment and mineralized nodule formation on rough and smooth 45S5 bioactive glass monoliths. *J Biomed Mater Res A*. 2004;**68**(4):640-50.
8. Karageorgiou V, Kaplan D. Porosity of 3D biomaterial scaffolds and osteogenesis. *Biomaterials*. 2005;**26**(27):5474-91.
9. Hutmacher DW. Scaffolds in tissue engineering bone and cartilage. *Biomaterials*. 2000;**21**(24):2529-43.
10. Bianco P, Riminucci M, Gronthos S, Robey PG. Bone marrow stromal stem cells: nature, biology, and potential applications. *Stem Cells*. 2001;**19**(3): 180-92.
11. Ciapetti G, Ambrosio L, Marletta G, Baldini N, Giunti A. Human bone marrow stromal cells: In vitro expansion and differentiation for bone engineering. *Biomaterials*. 2006;**27**(36):6150-60.
12. Kim DH, Lee H, Lee YK, Nam JM, Levchenko A. Biomimetic nanopatterns as enabling tools for analysis and control of live cells. *Adv Mater*. 2010;**22**(41): 4551-66.
13. International Organization for Standardization. Biological evaluation of medical devices: identification and quantification of degradation products from ceramics, ISO 10993-14:2001
14. Kim K, Dean D, Mikos AG, Fisher JP. Effect of initial cell seeding density on early osteogenic signal expression of rat bone marrow stromal cells cultured on cross-linked poly(propylene fumarate) disks. *Biomacromolecules*. 2009;**10**(7):1810-7.
15. Anokhina EB, Buravkova LB. [Heterogeneity of stromal precursor cells isolated from rat bone marrow]. *Tsitologiya*. 2007;**49**(1):40-7.
16. Huang Y, Siewe M, Madhally SV. Effect of spatial architecture on cellular colonization. *Biotechnol Bioeng*. 2006;**93**(1):64-75.
17. Lai JY, Lin PK, Hsiue GH, Cheng HY, Huang SJ, Li YT. Low Bloom strength gelatin as a carrier for potential use in retinal sheet encapsulation and transplantation. *Biomacromolecules*. 2009;**10**(2):310-9.
18. Huang Y, Siewe M, Madhally SV. Effect of spatial architecture on cellular colonization. *Biotechnol Bioeng*. 2006;**93**(1):64-75.

19. Davis JM. Ed. *Basic Cell Culture*. Oxford University Press, 2002. 408 p.
20. Gehrke P, Neugebauer J. Implant surface design: using biotechnology to enhance osseointegration. *Interview. Dent Implantol Update*. 2003;**14**(8):57-64.
21. Teixeira AI, Abrams GA, Bertics PJ, Murphy CJ, Nealey PF. Epithelial contact guidance on well-defined micro- and nanostructured substrates. *J Cell Sci*. 2003;**116**(Pt 10):1881-92.
22. Evans DJ, Britland S, Wigmore PM. Differential response of fetal and neonatal myoblasts to topographical guidance cues in vitro. *Dev Genes Evol*. 1999;**209**(7):438-42.
23. Karuri NW, Liliensiek S, Teixeira AI, Abrams G, Campbell S, Nealey PF, Murphy CJ. Biological length scale topography enhances cell-substratum adhesion of human corneal epithelial cells. *J Cell Sci*. 2004;**117**(Pt 15):3153-64.
24. Ducheyne P, Qiu Q. Bioactive ceramics: the effect of surface reactivity on bone formation and bone cell function. *Biomaterials*. 1999;**20**(23-24):2287-303.
25. Barinov SM, Shvorneva LI, Ferro D, Fadeeva IV, Tumanov SV. Solid solution formation at the sintering of hydroxyapatite-fluorapatite ceramics. *Sci Tech Adv Mater*. 2004; **5**(5-6): 537-41.
26. Danilchenko SN. Structure and properties of calcium apatite's regarding biomineralogy and biomaterial science (Review). *Visnyk SSU, Ser Fiz-Mat Nauk*. 2007; **2:33-59**.
27. Sudarsanan K, Mackie PE, Young RA. Comparison of synthetic and mineral fluorapatite, Ca₅(PO₄)₃F, in crystallographic detail. *Math Res Bull*. 1972; **7**(11):1331-7.
28. Okazaki M, Tohda H, Yanagisawa T, Taira M, Takahashi J. Differences in solubility of two types of heterogeneous fluoridated hydroxyapatites. *Biomaterials*. 1998;**19**(7-9):611-6.
29. Driessens FCM. Formation and stability of calcium phosphates in relation to the phase composition of the mineral in calcified tissues. In: *Bioceramics of calciumphosphate Eds de Groot K, CRC Press, Boca Raton, Florida 1983: 1-32*.
30. Gibson IR, Bonfield W. Novel synthesis and characterization of an AB-type carbonate-substituted hydroxyapatite. *J Biomed Mater Res*. 2002;**59**(4):697-708.
31. Lakhkar NJ, Lee IH, Kim HW, Salih V, Wall IB, Knowles JC. Bone formation controlled by biologically relevant inorganic ions: role and controlled delivery from phosphate-based glasses. *Adv Drug Deliv Rev*. 2013;**65**(4):405-20.
32. Thamilselvan V, Fomby M, Walsh M, Basson MD. Divalent cations modulate human colon cancer cell adhesion. *J Surg Res*. 2003;**110**(1):255-65.
33. Balaban NQ, Schwarz US, Riveline D, Goichberg P, Tzur G, Sabanay I, Mahalu D, Safran S, Bershadsky A, Addadi L, Geiger B. Force and focal adhesion assembly: a close relationship studied using elastic micropatterned substrates. *Nat Cell Biol*. 2001;**3**(5): 466-72.
34. Chrzanowska-Wodnicka M, Burridge K. Rho-stimulated contractility drives the formation of stress fibers and focal adhesions. *J Cell Biol*. 1996;**133**(6): 1403-15.
35. Hu DD, Barbas CF, Smith JW. An allosteric Ca²⁺ binding site on the beta3-integrins that regulates the dissociation rate for RGD ligands. *J Biol Chem*. 1996;**271**(36):21745-51.

Розпластування і проліферація стромальних клітин кісткового мозку при культивуванні на поверхні біоактивних склокристалічних матеріалів

V. V. Кірошка, О. В. Саввова, Ю. О. Божкова, І. В. Тамарина, О. І. Фесенко

Мета. Дослідити характер розпластування, структурну організацію цитоскелету, проліферацію стромальних клітин кісткового мозку при культивуванні на поверхні склокристалічних матеріалів (СКМ) різних за хімічним складом та розчинністю. **Методи.** В роботі було використано СКМ з різним співвідношенням СаО/Р₂О₅. Структуру актинового цитоскелету клітин було візуалізовано за допомогою фаллоїдину, кон'югованого з флуоресцентним барвником TRITC. Для оцінки проліферації клітин застосовували МТТ тест. **Результати.** Культивування клітин на СКМ серії В (атомне співвідношення Са/Р = 5 на поверхні), призводило до появи фібробластоподібних форм клітин із рівномірним розташуванням компонентів актинового цитоскелету в усьому обсязі цитоплазми. У цьому випадку динаміка

проліферації була аналогічною до такої, як при культивуванні на пластику. Зниження співвідношення Ca/P до 1,4 ÷ 2,58 серій А та С призводило до зменшення площі розпластування та індекса проліферації (у 2–3 рази) відносно контролю. **Висновки.** Основними факторами, які визначають поведінку клітин при взаємодії з СКМ, є розчинність матеріалу та співвідношення Ca/P на ростовій поверхні.

Ключові слова: склокристалічні матеріали, стромальні клітини кісткового мозку.

Распластывание и пролиферация стромальных клеток костного мозга при культивировании на поверхности биоактивных стеклокристаллические материалов

В. В. Кироска, О. В. Саввова, Ю. О. Божкова, И. В. Тамарина, А. И. Фесенко

Цель. Исследовать характер распластывания, структурную организацию цитоскелета, пролиферацию стромальных клеток костного мозга при культивировании на поверхности стеклокристаллических материалов (СКМ) различных по химическому составу и растворимости. **Методы.** В работе были использованы

СКМ, с различным соотношением CaO/P₂O₅. Структура актинового цитоскелета клеток была визуализирована при помощи фаллоидина, конъюгированного с флуоресцентным красителем TRITC. Для оценки пролиферации использовали МТТ тест. **Результаты.** Культивирование клеток на СКМ серии В (атомное соотношение Ca/P = 5 на поверхности), приводило к появлению фибробластоподобных форм клеток с равномерным расположением филаментов актинового цитоскелета по всему объему цитоплазмы. В этом случае динамика пролиферации была аналогичной таковой при культивировании на пластике. При снижении соотношения Ca/P до 1,4 ÷ 2,58 на поверхности СКМ серий А и С наблюдалось уменьшение площади распластывания и индекса пролиферации (в 2–3 раза) относительно контроля. **Выводы.** Основными факторами, определяющими поведение клеток при взаимодействии с СКМ, являются растворимость материала и соотношение Ca/P на ростовой поверхности.

Ключевые слова: стеклокристаллические материалы, стромальные клетки костного мозга.

Received 30.11.2016